Human Factors of a Global Society

A SYSTEM OF SYSTEMS PERSPECTIVE

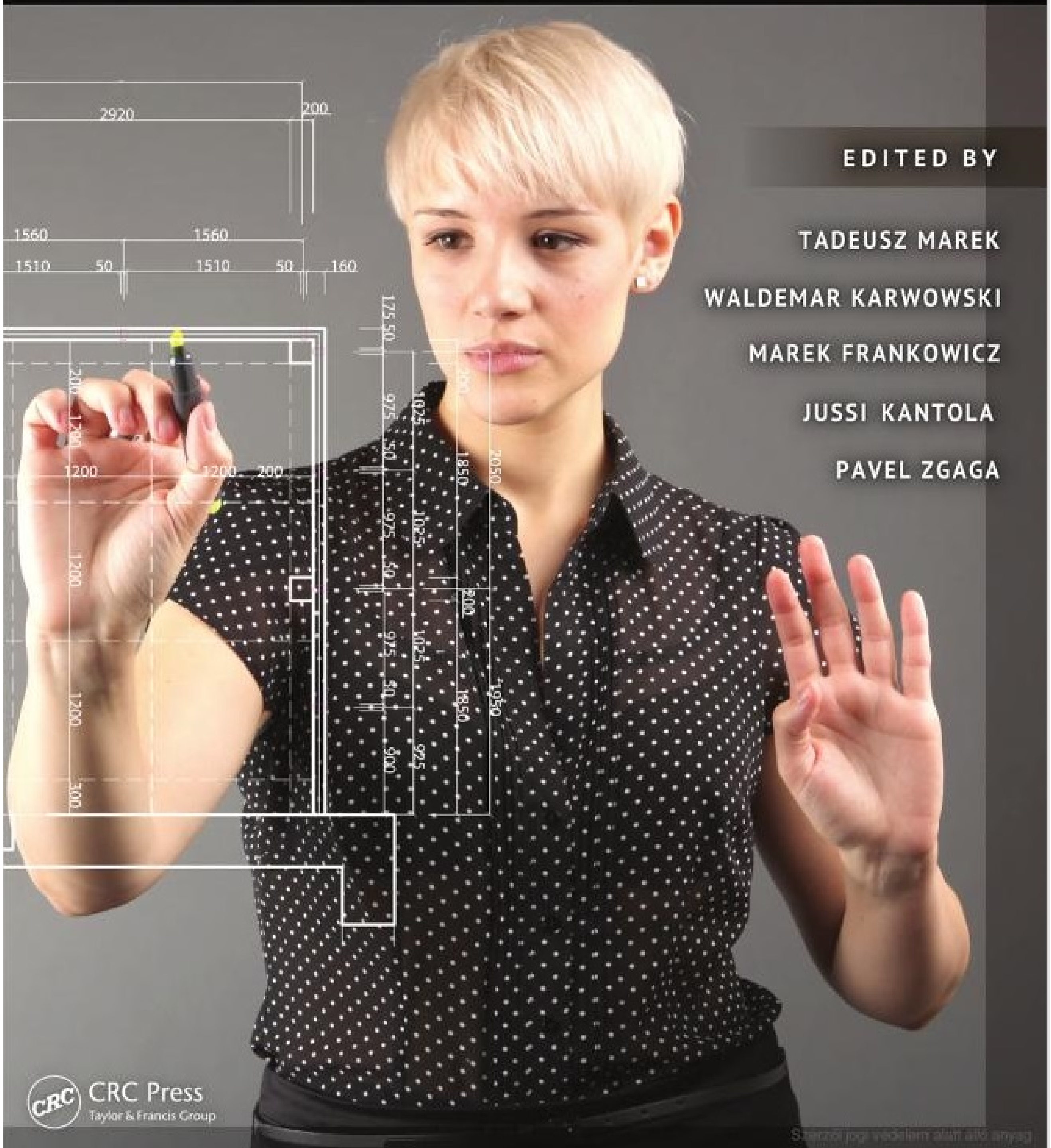

EDITED BY

TADEUSZ MAREK
WALDEMAR KARWOWSKI
MAREK FRANKOWICZ
JUSSI KANTOLA
PAVEL ZGAGA

CRC Press
Taylor & Francis Group

CRC Press
Taylor & Francis Group
6000 Broken Sound Parkway NW, Suite 300
Boca Raton, FL 33487-2742

Printed on acid-free paper
Version Date: 20131114

International Standard Book Number-13: 978-1-4665-7286-7 (Hardback)

Library of Congress Cataloging-in-Publication Data

Human factors of a global society : a system of systems perspective / edited by Tadeusz Marek, Waldemar Karwowski, Marek Frankowicz, Jussi Kantola, and Pavel Zgaga.
pages cm. -- (Ergonomics design and management theory and applications)
Includes bibliographical references and index.
ISBN 978-1-4665-7286-7 (hardcover : alk. paper)
1. Technology--Social aspects. 2. Human engineering. I. Marek, Tadeusz, 1951-

T14.5.H855 2014
920.8'2--dc23 2013041051

Visit the Taylor & Francis Web site at
http://www.taylorandfrancis.com

and the CRC Press Web site at
http://www.crcpress.com

Contents

14 Visualization of Multicriterial Classification

A Case Study

Péter Volf, Zoltán Kovács, and István Szalkai

CONTENTS

INTRODUCTION

Management of maintenance materials and parts (maintenance, repair, and operating [MRO] inventory) is a special field of material management concerning the nature of the role it plays in effective and efficient process operation. It is especially important because the forecast of the consumption of such materials is limited. MRO has a special feature, namely, the strong relationship between safety (reliability) and costs. Optimum operation can be achieved by a trade-off between them, based on systematic analysis.

Kennedy et al. (2002) differentiated the MRO inventories from the other types of manufacturing inventories such as works in process and finished products, based on their functionalities. They highlighted the function of MRO inventory, which is assigned not to be sold to a customer but to ensure the proper condition of equipment. That is why the nature of maintenance material management depends on the maintenance strategy, which is mostly a combination of following:

- Failure based: operation until a failure occurs, and then repair.
- Time based: examination and repair after a certain operational time or output.
- Condition based: repair is scheduled using information from condition monitoring.
- Maintenance prevention: construction and usage allows avoidance maintenance (maintenance-free operation).

The last three are preventive strategies. Forecast of material requirements is the most difficult in the case of failure-based strategy. When the cause of failure comes from a systematic effect like deterioration, the expected time between failures can be modeled by a normal or normal-like Weibull distribution. It allows the estimation of the increasing probability of failure as a function of the time since the last repair.

When failures are the results of nonsystematic effects, the distribution of failure-free operational times is (near) exponential, and failure can happen any time (memoryless process). This makes the demand forecast practically impossible. The number of failures during a long time interval might provide information about the expected demand.

Dhillon (2002) separates the MRO inventories in the above-mentioned way. There are MROs for routine and nonroutine maintenance tasks. However, the MRO inventories must be controlled in the most effective way; continuous availability is important in the first case. When controlling MRO inventories, there are four sorts of information needed:

- Importance of the inventory item
- The way it should be controlled
- Quantity to be ordered at one time
- Specific point in time to place an order

The answers to the first two questions are provided by the ABC analysis, which is one of the most frequently used methods to support the decision-making procedure in inventory management. It has many advantages, like easy usage and understandability. Its base is the famous Pareto observation, the so-called 80–20 rule. This rule serves as a basis for finding the cutoff figures between the groups according to the relative importance of the items (Deis 2008). The Pareto chart provides a perspicuous way of representing the three item categories—A, B, and C (Harry et al. 2010). This approach can be applicable only for classification based on one criterion, which is its most significant shortcoming.

Recognizing this problem, numerous methods have been developed to relieve the complex multicriterial decision-making situation in the last decades. These models, like the weighted linear optimization (Ramanathan 2006), the genetic algorithm (Guvemir and Erel 1998), the analytic hierarchy process (AHP) (Partovi and Burton 1993), and the fuzzy set theory (Chu et al. 2008), are capable of taking more than one criterion into account at the same time, enabling a more sophisticated analysis framework.

Alongside the development of new multicriterial models is a dramatic increase in their complexity. The way of improving these models focuses on their applicability, ignoring their understandability, which is one of the most important aspects of selecting a model for analysis. The proper visualization of each phase of the analysis and its results can relieve the implementation of complex models as well.

The visualization technique introduced in this chapter is based on the case-based distance model developed by Chen et al. (2008). In this sense, the present research is an extension of this model, improving the interpretation of its results. Hence, the main aim of this chapter is to demonstrate how visualization can help in understanding the structure of a complex inventory analysis model step by step.

The motivation was provided by Cho and Parlar (1991), who were among the first formulating critics on the lack of analysis of creation and application of new mathematical models and theories. Additionally, Scarf (1997) confirmed that too much emphasis is on developing new models and too little on application. That is why the results will be supported by a case study to facilitate the application of this mathematical model.

LITERATURE REVIEW

First, Flores and Whybark (1987) recognized that the classification of items is determined not only by one criterion but also by more specific characteristics like criticality, reparability, scarcity, substitutability, stockability, lead time, annual dollar usage, and commonality (Ramanathan 2006). However, increasing the number of dimensions in the analysis raises difficulties in interpretation of the results. This problem can be relieved by framing the decision situation and the problem embedded in it clearly through data visualization.

Lee et al. (2003) established a psychological framework to investigate the connection between the information coming from an artificial system and the human cognitive processes. The predecessor of this research had been conducted by Lee et al. (2003), who stated that viewing data visualization works as a channel conveying information between the two systems involved in their psychological framework. In particular, "data visualization has the potential to assist humans in analyzing and comprehending large volumes of data, and to detect patterns, clusters and outliers that are not obvious using non-graphical forms of presentation" (Lee et al. 2003).

Raising the number of factors (criteria) in inventory analysis leads to large, complex databases, whose elements are multivariate data. According to the Ward's (2008) definition, multivariate data are n-dimensional data consisting of more records and represented by an $m \times n$ matrix, where m is the number of data records and n is the value belonging to each variable or dimension.

There are many ways to represent multivariate data and the results of their analysis. Among these are the glyphs. Glyphs are visualization tools (Lee et al. 2003) that can show specific clusters or point at the interaction between variables. Starfield is another example for visualizing high-dimensional data, which is a two-dimensional scatter plot with the option to expand for more dimensions. Akcay et al. (2012) applied this tool for representing the two-dimensional results of a DEA model. Besides starfield, they implemented a tie graph for representing the same results. They argue that it is an effective tool for analysts to classify the data according to a criterion and uncover unrecognized patterns in the data envelopment analysis (DEA) results. Adler and Raveh (2008) conducted a research also in the topic of visualization opportunities of DEA approach. As a result they introduced a Co-plot method that is applicable for separating efficient units from outliers.

In general, Kim et al. (2008)—like Russel et al. (2008)—claimed that visualizing data provides important aids for decision makers to improve the decision-making process. Keim (2002) stated that the field of visualizing data is an important part of the research concerning computer science to amend the understandability of the data visually.

Concerning the inventory analysis in the field of inventory management, one of the main problems is that the large number of units can lead to an impracticable data set, which can make the application of the given model more complicated and can hinder the appropriate interpretation of the results. In this sense, the case-based distance model developed by Chen et al. (2008) excels compared to other models considering the structure of the model, because it involves an untapped opportunity in the view of interpretation of results. Namely, the process of determining the parameters of surfaces separating each group of storage keeping units (SKUs) is built in the model, and visualizing these surfaces can help to discover the magnitude of groups and the relationship between them.

MODEL CONSTRUCTION

The main aim of the case-based distance model is to classify the SKUs into categories according to the set Q of criteria. Let T be the set of the units (A^i) being analyzed, where $A^i \in T_g \subset T \mid g = A, B, C$ based on $q_j \in Q \mid j = 1, 2,\ldots, m$.

The minimum $\left(c_j^{\min}\right)$ and the maximum $\left(c_j^{\max}\right)$ values in positions A^- and A^+ form an interval (Chen et al. 2008). The Euclidean distances taken from these points determine the position of the given unit on criterion q_j.

Let the set $Z_{repg} \subseteq T_g \mid g = A, B, C$ be a subset of T_g that involves the units that principally represent the set T_g and $z_{repg}^r \in T_g \mid g = A,B,C$ is one of these units, where $c_j^{\min}(A^-) \le c_j\left(z_{repg}^r\right) \le c_j^{\max}(A^+)$ (Chen et al. 2008).

The case-based distance model is constructed for n dimensions, which, adopted on three criteria, becomes capable to be plotted as a *three*-dimensional coordinate system defined by the three elements of Q, where, respectively, radius vector $\overline{q_1}$ represents the x, $\overline{q_2}$ the y, and $\overline{q_3}$ the z axis.

After launching the normalization factor $d_j^{\max}$, the distance between the lower and upper bounds of the intervals changes (Chen et al. 2008).

$$d_j^{\max}(A^+;A^-) = \frac{\left(c_j^{\max}(A^+) - c_j^{\min}(A^-)\right)^2}{d_j^{\max}} = 1 \mid j = 1,2,3 \tag{14.1}$$

Since the distance between the lower and upper bound of the interval is equal to the absolute value of the radius vector on criterion j, the Euclidean distances taken from the points of comparison can be identified as the length of the radius vectors belonging to each unit. So the distance of $z^r_{repg} \in T_g$ from the upper limit of the interval on the second criterion is

$$d_2^+\left(A^+, z^r_{repg}\right) = \frac{\left(c_2^{\max}(A^+) - c_2\left(z^r_{repg}\right)\right)^2}{d_2^{\max}} = \frac{\left(\left\|\underline{q}^+_{r2}\left(0; c_2^{\max}(A^+) - c_2\left(z^r_{repg}\right); 0\right)\right\|\right)^2}{\left(\left\|\underline{q}_2^{\max}\left(0; c_2^{\max}(A^+) - c_2^{\min}(A^-); 0\right)\right\|\right)^2}$$

$$= \frac{\left(\sqrt{0^2 + \left(c_2^{\max}(A^+) - c_2\left(z^r_{repg}\right)\right)^2 + 0^2}\right)^2}{q_2^{\max}} = \frac{\left(c_2^{\max}(A^+) - c_2\left(z^r_{repg}\right)\right)^2}{q_2^{\max}}$$

where

$$d_2^{\max} = \left(c_2^{\max} - c_2^{\min}\right)^2 = \left(c_2^{\max}(A^+) - c_2^{\min}(A^-)\right)^2 = \left(\left\|\underline{q}_2^{\max}\left(0; \left(c_2^{\max}(A^+) - c_2^{\min}(A^-)\right); 0\right)\right\|\right)^2 = \left(\left\|\underline{q}_2^{\max}\right\|\right)^2 = q_2^{\max} \quad (14.2)$$

Based on the work of Chen et al. (2008), the weighted aggregation formulas of distance are

$$D^+\left(z^r_{repg}\right) = D^+\left(A^+_j; z^r_{repg}\right) = \sum_{j \in Q} w_j^+ \cdot d_j\left(z^r_{repg}\right)^+ = \sum_{j \in Q} w_j^+ \cdot \frac{\left(\left\|\underline{q}_j^+\left(x\left(z^r_{repg}\right); y\left(z^r_{repg}\right); z\left(z^r_{repg}\right)\right)\right\|\right)^2}{q_j^{\max}} \quad (14.3)$$

and

$$D^-\left(z^r_{repg}\right) = D^-\left(z^r_{repg}, A^-_j\right) = \sum_{j \in Q} w_j^- \cdot d_j\left(z^r_{repg}\right)^- = \sum_{j \in Q} w_j^- \cdot \frac{\left(\left\|\underline{q}_j^+\left(x\left(z^r_{repg}\right); y\left(z^r_{repg}\right); z\left(z^r_{repg}\right)\right)\right\|\right)^2}{q_j^{\max}} \quad (14.4)$$

respectively.

Note that depending on the point of comparison, we get two different sorting problems. Based on this fact, the visualization has to be separated likewise:

- If $c_j^{\min}(A^-)$ is the point of comparison, then we talk about *minimum transformation* in the minimum (distorted) space.
- If $c_j^{\max}(A^+)$ is the point of comparison, then we talk about *maximum transformation* in the maximum (distorted) space.

In this sense, the attribute "distortion" means that the values created by the value function $d_j\left(z^r_{repg}\right)$ from the original values are linear and nonlinear distorted, and this value transformation affects the sets and the shape of their separating surfaces, too.

Based on the linear and nonlinear transformations and their effects on the visualization, four different spaces ("worlds") can be identified:

1. Original space (Space 0)
2. Unit cube placed in "o" origin (Space 1)
3. Minimum (distorted) space (Space 2)
4. Maximum (distorted) space (Space 3)

Space 0: Let $P^i \in R^3$ be the point belonging to an SKU with the coordinates $P^i = \left(p_1^i, p_2^i, p_3^i\right)$, where $i = 1,2,\ldots,D$ and

$$\begin{cases} m_1 \le p_1^i \le M_1 \\ m_2 \le p_2^i \le M_2 \\ m_3 \le p_3^i \le M_3 \end{cases}$$

where (m_1, m_2, m_3) and (M_1, M_2, M_3) are the minimum and maximum values of the original coordinates, that is, $c^{\min}\left(c_1^{\min}; c_2^{\min}; c_3^{\min}\right)$ and $c^{\max}\left(c_1^{\max}; c_2^{\max}; c_3^{\max}\right)$.

Space 1: Linear transformation: $E = (\varepsilon_1, \varepsilon_2, \varepsilon_3) = \mathrm{T}(P)$, where

$$\varepsilon_1 = \frac{p_1 - m_1}{M_1 - m_1}, \varepsilon_2 = \frac{p_2 - m_2}{M_2 - m_2}, \varepsilon_3 = \frac{p_3 - m_3}{M_3 - m_3}$$

that is, in the case of $i = 1,2,\ldots,D$,

$$\varepsilon_1^i = \frac{p_1^i - m_1}{M_1 - m_1}, \varepsilon_2^i = \frac{p_2^i - m_2}{M_2 - m_2}, \varepsilon_3^i = \frac{p_3^i - m_3}{M_3 - m_3} \tag{14.5}$$

Consequently, the linear distorted coordinates are

$$E^i = \left(\varepsilon_1^i, \varepsilon_2^i, \varepsilon_3^i\right) = \mathrm{T}(P^i)$$

As a result, we get a unit cube placed in "o" origin.

Space 2: Minimum world (nonlinear transformation): $\xi = (\xi_1, \xi_2, \xi_3) = \Xi(E)$

Let

$$\begin{cases} \xi_1^i = \left(\varepsilon_1^i\right)^2 = \dfrac{\left(p_1^i - m_1\right)^2}{(M_1 - m_1)^2} \\ \xi_2^i = \left(\varepsilon_2^i\right)^2 = \dfrac{\left(p_2^i - m_2\right)^2}{(M_2 - m_2)^2} \\ \xi_3^i = \left(\varepsilon_3^i\right)^2 = \dfrac{(p_3^i - m_3)^2}{(M_3 - m_3)^2} \end{cases} \tag{14.6}$$

so in the case of $i = 1,2,\ldots,D$,

$$\xi^i = \left(\xi_1^i, \xi_2^i, \xi_3^i\right) = \Xi(\mathrm{T}(P^i))$$

Note that for $i = 1,2,\ldots,D$,

$$0 \le \xi_1^i \le 1, 0 \le \xi_2^i \le 1, 0 \le \xi_3^i \le 1$$

that is, the transformed points $\xi^i = d_j^-\left(z_{repg}^r\right)$ are in the *same* unit cube.

Space 3: Maximum world (nonlinear transformation): $\eta = (\eta_1, \eta_2, \eta_3) = \mathrm{H}(E)$

Let

$$\begin{cases} \eta_1^i = \left(1-\varepsilon_1^i\right)^2 = \dfrac{\left(M_1 - p_1^i\right)^2}{(M_1 - m_1)^2} \\ \eta_2^i = \left(1-\varepsilon_2^i\right)^2 = \dfrac{\left(M_2 - p_2^i\right)^2}{(M_2 - m_2)^2} \\ \eta_3^i = \left(1-\varepsilon_3^i\right)^2 = \dfrac{\left(M_3 - p_3^i\right)^2}{(M_3 - m_3)^2} \end{cases} \tag{14.7}$$

so in the case of $i = 1,2,\ldots,D$,

$$\eta^i = \left(\eta_1^i, \eta_2^i, \eta_3^i\right) = \mathrm{H}(\mathrm{T}(P^i))$$

Note, that in the case of $i = 1,2,\ldots,D$,

$$0 \le \eta_1^i \le 1, 0 \le \eta_2^i \le 1, 0 \le \eta_3^i \le 1$$

that is, the transformed $\eta^i = d_j^+\left(z_{rqpg}^r\right) \mid i = r$ are also in the unit cube.

It is easy to state that the relation between Space 2 and 3 is

$$\sqrt{\xi_1} + \sqrt{\eta_1} = 1, \sqrt{\xi_2} + \sqrt{\eta_2} = 1, \sqrt{\xi_3} + \sqrt{\eta_3} = 1 \tag{14.8}$$

Depending on which space we are analyzing for the position of the points P^i, the parameters searched are the following (Chen et al. 2008):

Space 2: $\xi^i = \left(\xi_1^i, \xi_2^i, \xi_3^i\right) = \Xi(\mathrm{T}(P^i))$

Weight vector: $w^- = \left(w_1^-, w_2^-, w_3^-\right)$;

Radii: R_B^- and R_C^-.

These parameters are given by the optimization model A^-MCABC expressed by the introduced transformation (Ξ) based on the work of Chen et al. (2008):

$$\min ERR = \sum_{r=1}^{n_A} \left(\alpha_C^r\right)^2 + \sum_{r=1}^{n_B} \left[\left(\alpha_B^r\right)^2 + \left(\beta_B^r\right)^2\right] + \sum_{r=1}^{n_C} \left(\beta_A^r\right)^2 \tag{14.9a}$$

where the conditions are

$$\sum_{j=1}^{3} w_j^- \cdot \xi_j^r + \alpha_C^r \le R_C^- \mid r = 1; 2; \ldots; n_C \tag{14.9b}$$

$$\sum_{j=1}^{3} w_j^- \cdot \xi_j^r + \alpha_B^r \le R_B^- \mid r = 1; 2; \ldots; n_B \tag{14.9c}$$

$$\sum_{j=1}^{3} w_j^- \cdot \xi_j^r + \beta_B^r \leq R_C^- \mid r = 1; 2; \ldots; n_B \tag{14.9d}$$

$$\sum_{j=1}^{3} w_j^- \cdot \xi_j^r + \beta_A^r \leq R_B^- \mid r = 1; 2; \ldots; n_A \tag{14.9e}$$

where

$$0 < R_C^- < 1, 0 < R_B^- < 1, R_C^- < R_B^-$$

$$-1 \leq \alpha_B^r \leq 0, \quad 0 \leq \beta_A^r \leq 1$$
$$-1 \leq \alpha_C^r \leq 0, \quad 0 \leq \beta_B^r \leq 1$$

$$w_j^- > 0; \sum_{j \in Q} w_j^- = 1 \tag{14.9f}$$

The model description of A^+MCABC in Space 3—$\eta^i = \left(\eta_1^i, \eta_2^i, \eta_3^i\right) = \mathrm{H}(\mathrm{T}(P^i))$—can be given in a similar way, where the parameters are
Weight vector: $w^+ = \left(w_1^+, w_2^+, w_3^+\right)$
Radii: R_A^+ and R_B^+ (Chen et al. 2008).

Visualization Method of Linear and Nonlinear Separating Surfaces

The nonlinear transformation implied by the value function $d_j\left(z_{repg}^r\right)$ on $z_{repg}^r = P_{repg}^i \mid i = r$ transformed the ellipsoids separating the set g into planes. In this way, the planes separating the sets in the distorted spaces can be given by the following formula:

Space 2: $\xi^i = \left(\xi_1^i, \xi_2^i, \xi_3^i\right) = \Xi(\mathrm{T}(P^i))$

$$\xi_3 = \frac{1}{w_3^-}\left(R_g^- - w_1^- \xi_1 - w_2^- \xi_2\right) \tag{14.10}$$

where $g = B^-, C^-$.

Space 3: $\eta^i = \left(\eta_1^i, \eta_2^i, \eta_3^i\right) = \mathrm{H}(\mathrm{T}(P^i))$

$$\eta_3 = \frac{1}{w_3^+}\left(R_g^+ - w_1^+ \eta_1 - w_2^+ \eta_2\right) \tag{14.11}$$

where $g = A^+, B^+$.

Note that due to the transformations above, the assumed relation between Space 2 and 3 cannot be assessed in distorted spaces. The design maps (DMs) have to return back to the original space in order to determine the interaction of the two classifications in the same space.

To get the three groups of SKUs and the ellipsoids separating them in the original space, execution of the inverse transformation is needed. Since $\xi^i = (\xi_1^i, \xi_2^i, \xi_3^i) = \Xi(\mathrm{T}(P^i))$ and $\eta^i = (\eta_1^i, \eta_2^i, \eta_3^i) = \mathrm{H}(\mathrm{T}(P^i))$ are monotone transformations of P^i, we can determine the ellipsoids separating the sets in the following way:

Space 2: $\xi^i = (\xi_1^i, \xi_2^i, \xi_3^i) = \Xi(\mathrm{T}(P^i)) \rightarrow \Xi(\mathrm{T}(P^i))^{-1} = (p_1^i, p_2^i, p_3^i) = P^i$.

The equation of planes dividing the sets in Space 2 is

$$\xi_3 = \frac{1}{w_3^-}\left(R_g^- - w_1^-\xi_1 - w_2^-\xi_2\right)$$

which can be reformed using Equation 14.6 into following formula:

$$\frac{(p_3 - m_3)^2}{(M_3 - m_3)^2} = \frac{1}{w_3^-}\left(R_g^- - w_1^- \frac{(p_1 - m_1)^2}{(M_1 - m_1)^2} - w_2^- \frac{(p_2 - m_2)^2}{(M_2 - m_2)^2}\right)$$

Expressing p_3, we can find the equation of the ellipsoids:

$$p_3 = m_3 + \sqrt{\frac{(M_3 - m_3)^2}{w_3^-}\left(R_g^- - w_1^- \frac{(p_1 - m_1)^2}{(M_1 - m_1)^2} - w_2^- \frac{(p_2 - m_2)^2}{(M_2 - m_2)^2}\right)} \tag{14.12}$$

where $g = B^-, C^-$.

In a similar way, in Space 3, the equation of the ellipsoids is

Space 3: $\eta^i = (\eta_1^i, \eta_2^i, \eta_3^i) = \mathrm{H}(\mathrm{T}(P^i)) \rightarrow \mathrm{H}(\mathrm{T}(P^i))^{-1} = (p_1^i, p_2^i, p_3^i) = P^i$

$$p_3 = M_3 - \sqrt{\frac{(M_3 - m_3)^2}{w_3^+}\left(R_g^+ - w_1^+ \frac{(M_1 - p_1)^2}{(M_1 - m_1)^2} - w_2^+ \frac{(M_2 - p_2)^2}{(M_2 - m_2)^2}\right)} \tag{14.13}$$

where $g = A^+, B^+$.

Note that in this case, the center of ellipsoids is the upper limit of the available values, that is, the *maximum value*.

Since the position of the points P^i representing the units in n-dimensional space is determined by the same criteria, the sets are able to be plotted in the same space, where their sections can be identified as the *nine sets before the reclassification*.

CASE STUDY

Data from analysis to be presented are from a heating power plant during the time period of June 1998–May 2011. During that time, 1595 items were in the MRO inventory. Recorded data were

- Volume (inv_vol)
- Time expired from the last outbound (last_out)
- Standard cost price (SCP)

After data screening (first eliminating items with 0 volume and then avoiding problems from different measure units), the sample size remained at 1064.

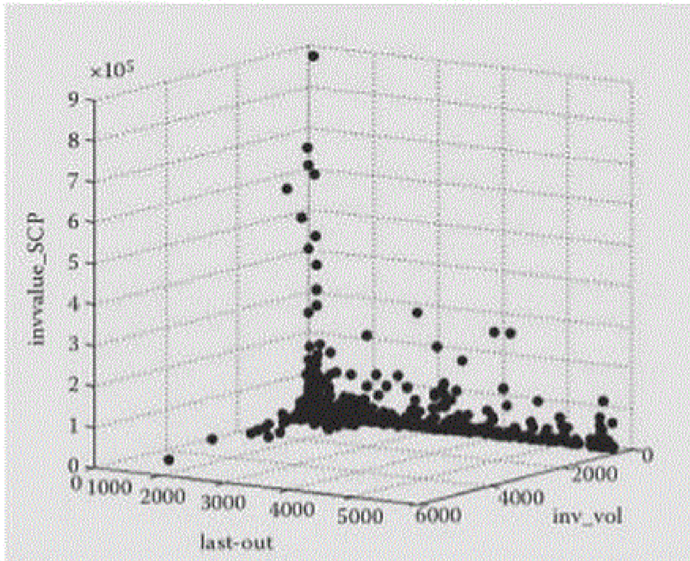

FIGURE 14.1 Distribution of item properties in 3-D coordinate system.

Figure 14.1 shows the positions of items in a 3-D coordinate system. The reason for 3-D visualization is that all analyses were carried out in a using multiple attributes, including correlation and cluster analysis. SPSS 18 statistics software has been applied to execute the systematic analyses.

Correlation and Cluster Analysis

Correlation analysis has been conducted to analyze the three classification-determining variables in terms of whether they fulfill the prerequisites of cluster analysis concerning the dependency.

The Spearman correlation coefficients show high values in two cases (Figure 14.2):

1. inv_vol – SCP
2. invvalue_SCP – SCP

Correlations			**inv_vol**	**SCP**	**last_out**	**invvalue_SCP**
Spearman's rho	inv_vol	Correlation coefficient	1.000	−.601**	−.271**	.017
		Significance (two-tailed)		.000	.000	.570
		N	1063	1063	1063	1063
	SCP	Correlation coefficient	−.601**	1.000	.073*	.755**
		Significance (two-tailed)	.000		.017	.000
		N	1063	1063	1063	1063
	last_out	Correlation coefficient	−.271**	.073*	1.000	−.114**
		Significance (two-tailed)	.000	.017		.000
		N	1063	1063	1063	1063
	invvalue_SCP	Correlation coefficient	.017	.755**	−.114**	1.000
		Significance (two-tailed)	.570	.000	.000	
		N	1063	1063	1063	1063

** Correlation is significant at the 0.01 level (2-tailed).

* Correlation is significant at the 0.05 level (2-tailed).

FIGURE 14.2 Correlation coefficients indicating the dependency between the classification-determining variables.

In the first case, there is a strong negative correlation, which means the higher the value of an item, the less of its volume is on hand. In the second case, since the value of inventory at SCP (invvalue_SCP) is a derived variable—a combination of SCP and volume— the high value of correlation is reasonable.

The high correlation of SCP with the other two variables does not allow us to apply the SCP in the analysis. There is only one variable that can substitute the SCB—the total value of a certain item on inventory (invvalue_SCP)—since it contains the effect of SCP (positive high correlation). Furthermore, since the value has a low correlation with volume and last move, instead of the initial three variables, the following three variables are the dimensions of cluster analysis:

- Volume (inv_vol)
- Time expired from the last outbound (last_out)
- Value (invvalue_SCP)

Due to the high number of MRO items, the *k*-means cluster analysis was reasonable. Keeping in mind the 80–20 rule, the *k*-means cluster analysis was repeated systematically in order to eliminate the outliers, of which classification is determined mainly by one variable. (Intermediate steps gave results with extreme shares, where small groups could be seen as outliners from a large group rather than independent groups.) As the result of this process, there remained a subset containing 531 items in the splitting shown in Figures 14.3 and 14.4.

The categories A, B, and C can be identified based on the characteristics of the previously formed groups by cluster anlysis. The key factor during the cluster analysis was the last_out; hence, the time elapsed from the last outbound determined the classification process. Its figures (minimum

Number of cases in each cluster		
Cluster	1	283.000
	2	100.000
	3	148.000
Valid		531.000
Missing		0.000

FIGURE 14.3 Cluster membership distribution in the screened subset.

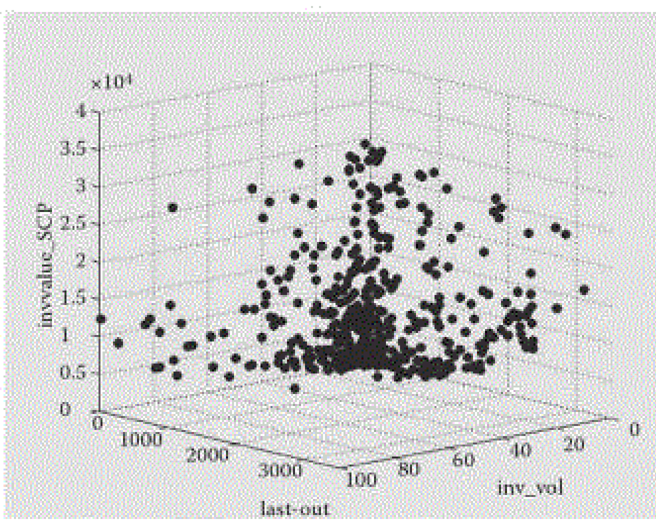

FIGURE 14.4 Distribution of item properties of the screened subset in 3-D coordinate system.

Group A
Descriptive statistics

	N	Minimum	Maximum	Sum	Mean	Standard deviation
inv_vol	100	1	89	792	7.92	12.303
last_out	100	210	3198	161,101	1611.01	675.180
invvalue_SCP	100	216	25,685	699,171	6991.71	6102.529
Valid N (listwise)	100					

Group B
Descriptive statistics

	N	Minimum	Maximum	Sum	Mean	Standard deviation
inv_vol	148	1	100	2175	14.70	18.596
last_out	148	6.5017	1940.5311	53,556.0908	361.8654	434.2664
invvalue_SCP	148	8392.15	30,060.00	2,495,924.59	16,864.3553	6416.1419
Valid N (listwise)	148					

Group C
Descriptive statistics

	N	Minimum	Maximum	Sum	Mean	Standard deviation
inv_vol	283	1	94	3329	11.76	16.347
last_out	283	0.5922	886.2879	39,176.2599	138.4320	166.7914
invvalue_SCP	283	49.2800	9218.0400	858,107.5500	3032.1821	2419.6868
Valid N (listwise)	283					

FIGURE 14.5 Descriptive statistics of variables in each cluster.

and maximum values, mean, deviation—Figure 14.5) are continuously decreasing from group A to group C, while the difference between the figures of volume (inv-vol) in each groups are not significan,t and no trend can be recognized in the case of value (invvalue_SCP).

Visualization of the Classification of MRO

Correlation analysis provided the three independent variables that can be taken into account to determine the categories of MRO items. Cluster analysis as a part of the screening process has been used to make an estimation for the groups of items advanced. As a result, the original set has been reduced by eliminating the outliers to come up with a subset consisting of 531 items. Applying the $A^{-}MCABC$ and $A^{+}MCABC$ models, we can obtain the weights for each criterion and the cutoff values for radii in both spaces:

***Space 2** (minimum world):* $\xi^i = \left(\xi_1^i, \xi_2^i, \xi_3^i\right) = \Xi(\mathrm{T}(P^i))$
Weight vector: $w^- = (0.243331; 0.01; 0.746669)$;
Radii: $R_B^- = 0.001406478$ and $R_C^- = 0.0001781243$.

***Space 3** (maximum world):* $\eta^i = \left(\eta_1^i, \eta_2^i, \eta_3^i\right) = \mathrm{H}(\mathrm{T}(P^i))$
Weight vector: $w^+ = (0.1620604; 0.08130314; 0.7566364)$;
Radii: $R_A^+ = 0.982917$ and $R_B^+ = 0.9410705$.

Lingo and MATLAB® software were used to calculate the necessary model parameters and to plot the surfaces.

Since the linear and nonlinear transformations affect not only the coordinates but also the separating surfaces, substituting into Equations 14.10 and 14.11 can confirm that the previously assumed nonlinear surfaces (ellipsoids) are planes in the distorted spaces (Figures 14.6 and 14.7).

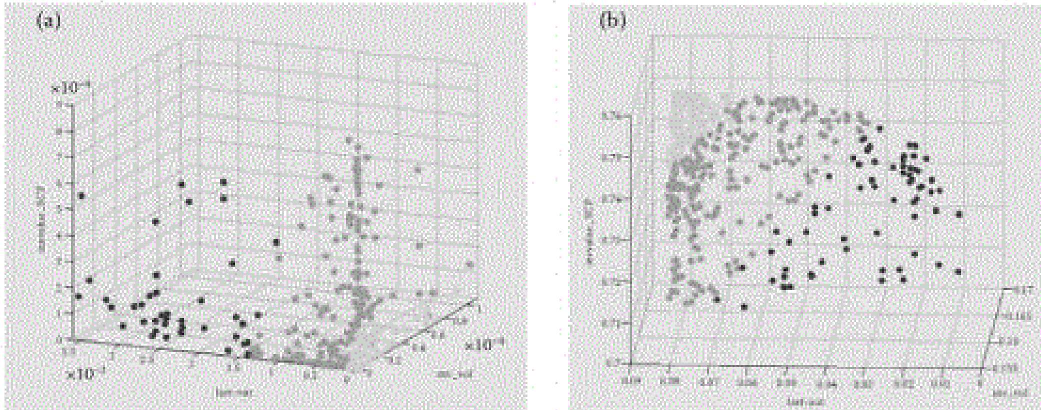

FIGURE 14.6 Visualization of groups in Space 2 and 3 (black, group A; gray, group B; light gray, group C).

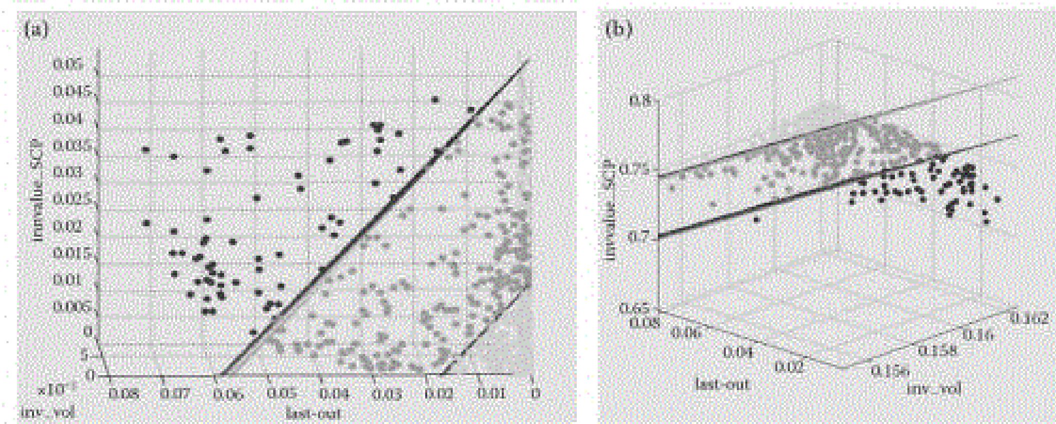

FIGURE 14.7 Visualization of groups and planes separating them in Space 2 and Space 3.

The inverse transformation ensures the feasibility of representation of the real categories of items and their separating nonlinear surfaces (substituting into Equations 14.12 and 14.13) in the same space. Figures 14.8 and 14.9 demonstrate the positions of the groups in the three-dimensional coordinate system. The relative proportion of magnitudes and density of groups can provide the same information about classification as the distribution in the case of Pareto analysis.

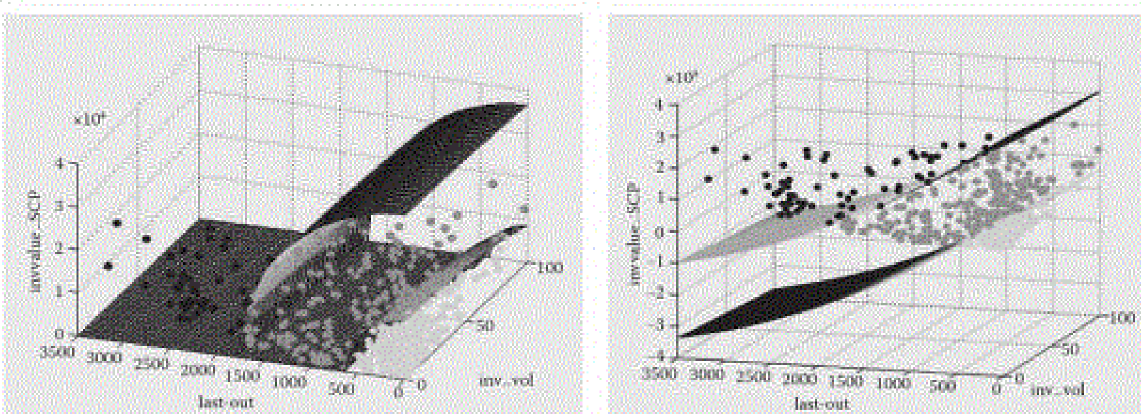

FIGURE 14.8 Visualization of groups of SKUs and ellipsoids bounding them in the minimum and maximum world using the original coordinates.

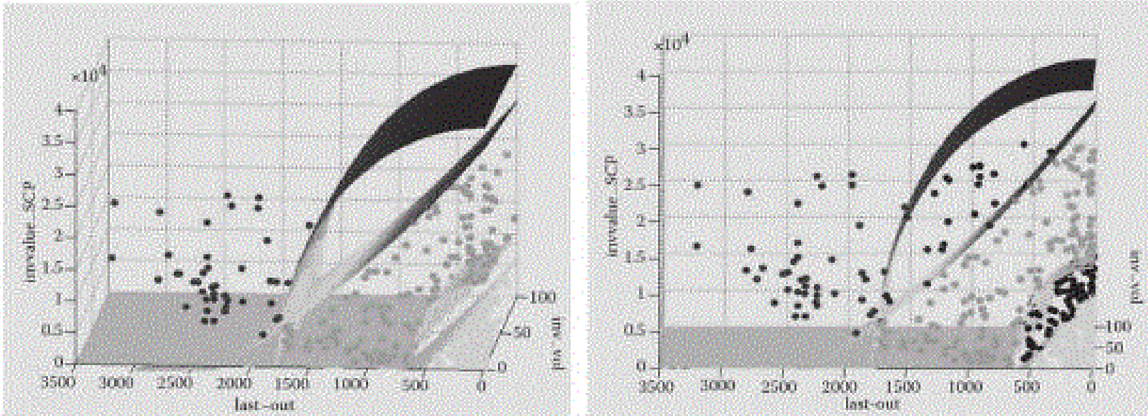

FIGURE 14.9 Visualization of classification results in one space (Space 0).

As a result, five categories have been identified (right side of Figure 14.9). Three of them are unambiguous—having the same classification results irrespective of the points of comparison (AA, BB, CC—left side of Figure 14.9). However, there are two item categories whose positions raise difficulties relating to the interpretation of classification results. Two principles can support the decision in this case. First, if the basic task is to identify the "best-performing" items (with the highest values), then the classification results of the maximum world have to be considered, and conversely, if the basic task is to identify the "worst-performing" items (with the lowest values), then the classification results of the minimum world have to be considered, which is the second principle.

CONCLUSION

The case study pointed out that the analysis of MRO inventories requires more serious methodology than analysis of other inventories does. The combination of systematic and nonsystematic effects raised difficulties in defining groups of material. Taking more properties into consideration increases the complexity of the problem. However, to alleviate the decision process or situation in the case of a sorting problem, visualization of multicriterial ABC analysis requires a sophisticated mathematical apparatus, for which an example has been provided.

In the presented case, a strong correlation was found between the unit cost (originated from purchase price) and volume.

It was also our experience that cluster analyses can be applied in an iterative way in order to make a distinction between outliers and groups.

After implementing statistical methods such as correlation analysis and cluster analysis, the presented case study gave an example of the application of visualization of a complex multicriterial classification technique (case-based distance model).

Next, researches will discover the type of inventories for which the presented methods (MCABC, cluster analysis, visualization) are applicable.

REFERENCES

Adler, N., Raveh, A. (2008): Presenting DEA graphically. *Omega* 36, 715–729.

Akcay, A.E., Gurdal Ertek, G., Buyukozkan, G. (2012): Analyzing the solutions of DEA through information visualization and data mining techniques: SmartDEA framework. *Expert Systems with Applications* 39, 7763–7775.

Chen, Y., Li, K.W., Kilgour, D.M., Hipel, K.W. (2008): A case-based distance model for multiple criteria ABC analysis. *Computers and Operations Research* 35, 776–796.

Cho, D.I., Parlar, M. (1991): A survey of maintenance models for multi-unit systems. *European Journal of Operational Research* 51, 1–23.

Chu, Ch.W., Liang, G.S., Liao, Ch.T. (2008): Controlling inventory by combining ABC analysis and fuzzy classification. *Computers and Industrial Engineering* 55, 841–851.

Deis, P. (2008): *Production and Inventory Management in the Technological Age*. Essex of Oak Park, Agoura Hills, CA.

Dhillon, B.S. (2002): *Engineering Maintenance: A Modern Approach*. CRC Press LLC, FL.

Flores, B.E., Whybark, D.C. (1987): Implementing multiple criteria ABC analysis. *Journal of Operations Management* 7(1–2), 79–85.

Guvemir, H.A., Erel, E. (1998): Multicriteria inventory classification using a genetic algorithm. *European Journal of Operational Research* 105, 29–37.

Harry, M.J., Mann, P.S., De Hodgins, O.C., Hulbert, R.L., Lacke, C.J. (2010): *Practitioner's Guide to Statistics and Lean Six Sigma for Process Improvements*. John Wiley and Sons, Hoboken, NJ.

Keim, D.A. (2002): Information visualization and data mining. *IEEE Transactions on Visualization and Computer Graphics* 8(1), 1–8.

Kennedy, W.J., Patterson, J.W., Fredendall, L.D. (2002): An overview of recent literature on spare parts inventories. *International Journal of Production Economics* 76, 201–215.

Kim, Y.G., Suh, J.H., Park, S.C. (2008): Visualization of patent analysis for emerging technology. *Expert Systems with Applications* 34(3), 1804–1812.

Lee, M.D., Butavicius, M.A., Reilly, R.E. (2003): Visualizations of binary data: A comparative evaluation. *International Journal of Human-Computer Studies* 59, 569–602.

Partovi, F.Y., Burton, J. (1993): Using the analytic hierarchy process for ABC analysis. *International Journal of Production and Operations Management* 13, 29–44.

Ramanathan, R. (2006): ABC inventory classification with multiple-criteria using weighted linear optimization. *Computers and Operations Research* 33, 695–700.

Russell, S., Gangopadhyay, A., Yoon, V. (2008): Assisting decision making in the event-driven enterprise using wavelets. *Decision Support Systems* 46(1), 14–28.

Scarf, P.A. (1997): On the application of mathematical models in maintenance. *European Journal of Operational Research* 99, 493–506.

Ward, M.O. (2008): Multivariate data glyphs: Principles and practice. *Handbook of Data Visualization*. Springer, Berlin, 179–198.